Fracture initiation and propagation in unidirectional CF composites based on thermoplastic acrylic resins

Tommaso Pini, Francesco Caimmi, Francesco Briatico-Vangosa, Roberto Frassine, Marta Rink

Politecnico di Milano, Department of Chemistry, Materials and Chemical Engineering ”Giulio Natta”, Piazza Leonardo da Vinci 32, I-20133, Milano, Italy

Engineering Fracture Mechanics 184 (2017) pp. 51-58

Abstract

The fracture behaviour of continuous unidirectional carbon fibre composite materials prepared adopting two, one plain and one rubber toughened, thermoplastic acrylic resins as matrices was investigated as a function of temperature and displacement rate. The contributions to fracture toughness of composites given by the matrix and the fibre related mechanisms was analysed by comparing results obtained at crack initiation and during crack propagation stages. It was verified that the transfer of matrix toughness into the composite is only partial when the matrix process zone size is comparable to the interlaminar matrix layer thickness. The effectiveness of fibre bridging mechanism was found to be related to the interfacial strength between the matrix and the fibre.

This is the post-print author version of this work.

Publisher’s version of the article is available at http://doi.org/10.1016/j.engfracmech.2017.08.023

© <2017>. This manuscript version is made available under the CC-BY-NC-ND 4.0 license
http://creativecommons.org/licenses/by-nc-nd/4.0/

Fracture initiation and propagation in unidirectional CF composites based on thermoplastic acrylic resins

T. Pini[a,*], F. Caimmi[a], F. Briatico-Vangosa[a], R. Frassine[a], M. Rink[a]

[a]*Politecnico di Milano, Department of Chemistry, Materials and Chemical Engineering "Giulio Natta", Piazza Leonardo da Vinci 32, I-20133, Milano, Italy*

Abstract

The fracture behaviour of continuous unidirectional carbon fibre composite materials prepared adopting two, one plain and one rubber toughened, thermoplastic acrylic resins as matrices was investigated as a function of temperature and displacement rate. *The contributions to fracture* toughness of composites given by the matrix and the fibre related mechanisms was analysed by comparing results obtained at crack initiation and during crack propagation stages. It was verified that the transfer of matrix toughness into the composite is only partial when the matrix process zone size is comparable to the interlaminar matrix layer thickness. The effectiveness of fibre bridging mechanism was found to be related to the interfacial strength between the matrix and the fibre.

Keywords:

matrix toughness, viscoelasticity, thermoplastic composites, fibre bridging, infusion moulding

1. Introduction

Composite materials are widely used in all those applications where a reduction of weight and high performance are desired. Growing interest has been put on composite materials based on thermoplastic polymeric matrices due to the advantages that come from the adoption of this class of materials: the parts can be, for example, welded, thermoformed and recycled [1]. Further, in comparison with thermosets, thermoplastic polymers show higher ductility and toughness. The

*Corresponding author

Email address: tommaso.pini@polimi.it (T. Pini)

major drawback to adoption of thermoplastics as matrices for composite materials is the difficulty to achieve good impregnation of the fibres during processing, due to the high melt viscosity of these materials. Production methods specific to this class of materials, which are often time and money consuming, appear necessary to reduce the distance that the resin has to flow through the fibres [2, 3, 4, 5]. A cost saving solution to this issue could be the adoption of a processing technique based on in-situ polymerization [6, 7]. In the case of infusion moulding, for example, the low viscosity monomers can flow through the fibres achieving good impregnation after which the polymerization reaction takes place.

Matrix toughness has a fundamental role in determining interlaminar mode I fracture toughness of a composite material which is a limiting property of a composite from a durability and damage tolerant approach point of view. The resistance to interlaminar crack growth of different composite materials has been found to be in some cases higher than that of the neat matrix (as in [8] for different epoxies and carbon fibres (CF) and in [9] for PEEK/CF) and in some cases lower (as in [10] for PEEK/CF and epoxy/CF and in [11] for PEI/CF). Fracture toughness of a composite is actually related to both the toughness of the matrix [8, 12, 13] and several energy dissipating mechanisms more related to the fibres or to their interaction with the matrix, such as fibre breakage, fibre pull-out, matrix/fibre debonding, fibre bridging and formation of side cracks [10]. Concerning the toughness of the matrix, this can be, partially or fully, transferred into the composite. Usually, more brittle matrices are able to transfer all their toughness into the composite while, in the case of more ductile matrices only a fraction of matrix toughness actually contributes to crack growth resistance in the composite [12, 13, 14]. It is quite challenging, in order to optimise the composite performance, to distinguish between the different mechanisms that concur to the fracture toughness of a laminate. It is commonly accepted that at crack initiation the major contribution is given by matrix toughness while the difference between fracture toughness at initiation and propagation stages is largely determined by the fibre bridging mechanism, which is present only during propagation [14, 15].

In the present work, the fracture behaviour of unidirectional continuous carbon fibre composites having two different acrylic thermoplastic resins as matrices was investigated. Since the matrices can be polymerized in-situ, infusion moulding was adopted as processing technique. The effect

of matrix viscoelasticity on the fracture behaviour of the composite was investigated, measuring interlaminar fracture toughness at different temperatures and displacement rates, as in [9, 11]. The different contributions to fracture toughness of the laminates were investigated considering both crack initiation and crack propagation stages.

2. Materials

Two different acrylic polymers, both produced by Arkema, were adopted as matrices, namely:

- Elium®, named E, having a glass transition temperature, T_g, of 127 °C.
- Elium Impact®, named EI, similar to the previous one, toughened with 10 wt% of an acrylic block copolymer (Nanostrength®). The rubbery structures produced have a size below 50 nm. Two glass transition temperatures are observed at -25 °C and 130 °C respectively.

Glass transition temperature was determined through Dynamical Mechanical Analysis, considering the peak of the $\tan\delta$ vs. temperature curve. To this aim, a TA RSA-3 DMA was used to perform a temperature ramp at the heating rate of 2 °C/min at the fixed frequency of 1Hz. The fibres used were T700 12 K continuous unidirectional carbon fibres, held together by glass fibre stitches. Composites were prepared by infusion moulding. After infusion, for composites prepared with E resin, polymerization took place at room temperature for 24 hours with an additional thermal treatment of 1 hour at 80 °C and 1 hour at 120 °C. For EI-based composites a thermal cycle of 5 hours at 80 °C and 1.5 hours at 125 °C was applied. The polymerization conditions chosen were the same adopted in [16] to prepare neat resin samples with which the fracture behaviour of the composites was compared. Nevertheless, some difference in the polymerization conditions could occur due to the different thermal conductivity of the fibres. Fibre volume fraction was evaluated, having previously measured the densities of the resin and the fibres, from the fibre weight content, which was measured by the resin burning method. It resulted to be about 60 %.

3. Test methods

Interlaminar fracture toughness was evaluated as the strain energy release rate, G_{Ic}, according to ISO 15024:2001 standard [17]. Double cantilever beam specimens (Fig. 1) having dimensions

of 190x20x3 mm and 190x20x10 mm, for composites having untoughened (E) and toughened (EI) matrix respectively, were cut from plates produced by infusion moulding. These dimensions differ from those given in the standard but from preliminary runs of tests it was found necessary, especially in the case of the composites based on the toughened resin, to adopt thicker specimens in order to avoid kinking and breakage of the arms of the specimens. In all the specimens an initial delamination 60 mm long was introduced by placing a thin (13 μm) PTFE release film on the laminate midplane. The ends of the specimen containing the delamination were sanded and then cleaned with acetone in order to bond load blocks with an epoxy adhesive. One side of the specimen was painted white with dark marks at regular intervals so as to ease the individuation of the crack tip and the measurement of the crack length during crack propagation.

A first stage of loading (pre-cracking) was performed at a constant displacement rate of 2 mm/min in order to obtain a natural crack up to 3-4 mm ahead the film insert. Then, the actual tests were carried out up to 90-110 mm of further crack propagation at constant displacement rates varying from 0.2 to 200 mm/min and temperatures between 0 and 60 °C. Tests were performed on an Instron 1185 dynamometer equipped with a 10 kN load cell and a thermostatic cabinet and, only at 23 °C, on a MTS 831.50 servohydraulic dynamometer that can reach crosshead displacement rates up to 8 m/s.

Strain energy release rate was evaluated as

$$G_{Ic} = \frac{3P_c\delta}{2W\,(a + |\Delta|)}\frac{F}{N} \tag{1}$$

where P_c is the fracture load, δ the displacement, W the specimen width, a the crack length and Δ, F and N are corrective factors for beam root rotation, large displacements and load blocks respectively as described in [17]. Tests were video-recorded and crack length was measured.

Fracture toughness at initiation, $G_{Ic,init}$, was determined by visual observation of the beginning of crack growth, which is the VIS point reported in [17]. The corresponding time is the crack initiation time, t_{init}. It should be noticed that the two other approaches described by the standard (deviation from linearity (NL) and 5% offset or maximum load (5%/MAX)) gave similar results. The usual ranking was generally observed, with fracture toughness at 5%/MAX greater than that at VIS, which in turn was greater than that at NL. With respect to VIS values, NL are about 14

% lower and 5%/MAX are about 18 % higher. Fracture toughness during propagation, $G_{Ic,prop}$, was determined as the average of the values recorded over a wide range of crack growth where toughness is fairly constant. In the same range, crack propagation speed, $\dot{a}$, was evaluated as the slope of crack length vs. time curves. An example of an R-curve, in which fracture toughness is plotted vs. crack length, is given in Fig. 2 where the point at which $G_{Ic,init}$ was determined and the propagation region over which the average value of $G_{Ic,prop}$ was evaluated are indicated. The difference between fracture toughness during propagation and at initiation, ΔG, is also shown in Fig. 2.

4. Results

Results of fracture tests performed at different temperatures and displacement rates for the composites with the two different matrices (E and EI) are given in Fig. 3 and Fig. 4 for crack initiation ($G_{Ic,init}$ vs. t_{init}) and crack propagation ($G_{Ic,prop}$ vs. $\dot{a}$) respectively. Each point in each plot corresponds to a specimen. Under the hypothesis that the time dependence of the mechanical response of a composite is governed by the viscoelasticity of the matrix, time-temperature equivalence was applied: isothermal fracture toughness values were shifted along the logarithmic initiation time or crack speed axis using the shift factors relevant to the matrices previously obtained in [16] and reported in Table 1, as previously done in [11], to which the reader is referred for a discussion of the validity of the approach. The master curves obtained for crack initiation and for crack propagation are reported in Fig. 5 and Fig. 6 respectively together with those of the relevant matrices previously obtained in [16].

A good superposition of the curves can be observed in Fig. 5 and Fig. 6, in the case of EI composite for which a rate dependence of fracture toughness was found. Concerning crack initiation, from Fig. 5 it can be observed that in the case of E resin while the matrix fracture toughness decreases as initiation time increases, in agreement with viscoelastic fracture theories as shown in [16], the composite fracture toughness is constant irrespective of crack initiation time. For EI resin the matrix shows an increasing trend for $G_{Ic,init}$ vs. t_{init} due to a change in damage mechanism as reported in [16] and in this case the composite shows a quite similar trend. Further, in the case of E resin the composite is tougher than the matrix, while the opposite occurs in the case of the EI resin.

With regard to crack propagation, Fig. 6 shows that both composites, in all tested conditions, have a higher fracture toughness than that of their relevant matrices. Also during propagation, as for fracture toughness at crack initiation, the two matrices show opposite trends. For the untoughened resin, E, fracture toughness of the matrix increases as crack speed increases while for the composite it is almost constant. In the case of the toughened resin the fracture toughness decreases as crack propagation speed increases for both the matrix and the composite.

5. Discussion

The discussion of these results will be presented separately for fracture initiation and propagation stages.

5.1. Fracture initiation

As mentioned in the introduction, fracture initiation results (Fig. 5) can give a better indication on the fraction of matrix toughness that is translated into the composite, although the contribution of other mechanisms cannot be excluded. The fact that composite fracture toughness is higher than that of the matrix, as in the case of E composite, is a necessary but not sufficient condition to infer a complete transfer of matrix toughness into the composite. Nevertheless, the composite toughness does not appear to depend on initiation time as the matrix does, thus it is reasonable to assume that, in the time range investigated, fracture toughness is dominated by the energy dissipating mechanisms linked to the presence of the fibres. As is reported further on (sec. 5.2), the fibre-matrix interface is weak, therefore fracture probably occurs along this interface rather than within the matrix, resulting in a higher but not rate dependent fracture toughness for the composite.

The EI composite shows a lower fracture toughness than its relevant matrix, indicating that the transfer of toughness of the latter into the composite is only partial but a contribution to toughness of mechanisms linked to the fibres can not be excluded. For both matrix and composite $G_{Ic,init}$ vs. t_{init} curves show a decreasing trend indicating that all mechanisms involved have a similar rate dependence.

Concerning the transfer of the matrix toughness into the composite, this is related to the process zone in the resin-rich layer containing the initial notch plane whose development can be hindered

by the fibres in the adjacent plies, as reported in [9, 11, 12, 14]. The thickness of the interlaminar resin layer was, thus, compared with the size of the process zone of the relevant matrix. This thickness was measured from cross-sections cut from pristine DCB specimens (2 specimens for each material) which were polished and observed with an optical microscope in different positions of each lamina. The critical Crack Tip Opening Displacement (CTOD) of the neat matrices was considered as a measure of the size of the process zone in the direction perpendicular to the crack plane and its measurement was carried out at different temperatures by means of Digital Image Correlation. A complete description of the measuring technique is reported in [16].

The thickness of the resin rich layer was more or less the same between all the different plies and along the specimens (slightly different between the two materials). The average value of the interlaminar matrix layer thickness of the two composites is given in Fig. 7 in comparison with the CTOD values obtained at different temperatures for the relevant matrices. The same results are visually represented in Fig. 8. It can be observed that in the case of E matrix the CTOD is constant with temperature and is about one order of magnitude smaller than the thickness of the interlaminar matrix layer. In the case of the toughened matrix CTOD increases as temperature increases but even the smallest value is comparable with the thickness of the interlaminar resin-rich layer confirming that the presence of the fibres probably hindered the full development of the process zone.

5.2. Fracture propagation

It can be observed from Fig. 6 that both composites showed a higher fracture toughness than that of their relevant matrices over the crack speed range investigated. It is useful to discuss the results by comparing them with those obtained at crack initiation. The increase of fracture toughness, ΔG (Fig. 2), between the toughness at crack initiation, $G_{Ic,init}$, and the steady-state value reached during crack propagation, $G_{Ic,prop}$, is the energy dissipated through fibre bridging mechanism which is not active at initiation. Fig. 9 shows ΔG as a function of crack propagation speed for the two materials. It can be observed that in the case of E composite the increase of fracture toughness is quite small and not dependent on crack propagation speed. On the other hand, ΔG is considerable in the case of EI composite and a strong effect of rate is observed. The contribution

to toughness from the fibre bridging mechanism depends on the number of bridging fibres per unit area and on the energy necessary to pull off the fibre from the matrix and in some cases also to pull them out/break them [10].

The fracture surfaces from the propagation region of almost all the specimens tested were observed with a stereomicroscope at low magnification. Both surfaces of each specimen were observed. The images of selected specimens are reported in Fig. 10 and Fig. 11 for E and EI composites respectively. In all images the propagation direction is from left to right. A reliable quantification of the number of fibres debonded from the matrix was not achieved from these images, thus only qualitative considerations were made. For both materials it seems that the amount of debonded fibres (shiny white thin lines in the images) is neither affected by temperature nor an effect of displacement rate was observed from images not reported here. Moreover, the density of debonded fibres seems to be similar for E and EI composites. The white, regular, vertical stripes in Fig. 10 and Fig. 11, which are the stitches adopted to hold together the carbon fibres, appear to be different on the surfaces of the two materials: in all the E composite specimens observed, the regular pattern of the stitches is clearly visible after testing (see Fig. 10) while in the case of EI composites, only few stitches are observable in Fig. 11, indicating that probably there is still some matrix covering the fracture surfaces. The same specimens reported in Fig. 10 and Fig. 11 were metallized and observed with a Zeiss EVO 50 Scanning Electron Microscope (SEM). Observation of the surfaces at low (75x) magnification confirmed that the density of the fibres detached from the surface does not appear significantly affected by the testing temperature and it is similar for the two materials investigated. The stitches, almost invisible from Fig. 11 in the case of EI composite, were observed with SEM confirming that they are covered by a matrix layer. Images taken at 5000x magnification are reported in Fig. 12 and Fig. 13 for E and EI composites respectively. The appearance of the fibres is quite different for the two materials. In the case of the untoughened resin based composites, at all temperatures (rates) tested, fibres appear naked with a smooth surface, as also fibre tracks do. This indicates that fracture occurs at the fibre matrix interface as a consequence of a poor interfacial strength [18]. Contrarily, images from Fig. 13 show large amount of matrix still attached to the fibres for EI composite, indicating that the fracture occurred partially cohesively in the matrix rather than only at the interface. Further, the deformation of the matrix seems larger as

temperature increases.

Being the number of debonded fibres similar for the two composites it is reasonable to assume that the different toughness increase (ΔG) for the two composites can be ascribed to the fact that they have different debonding mechanisms requiring different amounts of energy to free the fibres from the matrix. For the composite based on the plain resin the energy contribution due to fibre bridging is low due the low interfacial strength as observed from the TEM micrographs and resulted independent of rate or temperature. For the composite made with the toughened polymer, ΔG is considerable and has a rate (and temperature) dependence similar to that of the matrix. This is consistent with the fact that the mechanism necessary to make a fibre debond and bridge the crack involves mainly fracture within the matrix rather than interfacial failure and fibre pull-out, as also suggested by SEM images (Fig. 13).

The assumption of a different interfacial toughness for the two different matrices should be independently validated. This is outside of the scope of the present work and left as a refinement for a future separate work.

6. Conclusions

In a previous paper [16] the time dependence fracture toughness of two acrylic resins, one plain and one toughened, was studied. The former showed a behaviour consistent with viscoelastic fracture theories while that of the latter reflected a change in the deformation mechanisms. In this research the same resins were used as matrices for unidirectional CF composites and fracture behaviour at both initiation and propagation stages was analysed. The following conclusions coud be drawn:

(i) regarding fracture initiation, it was found that the transfer of the matrix toughness into the composite is possible if the process zone of the matrix in the composite can fully develop. Direct measurements showed that, when the size of the process zone and that of the interlaminar matrix region are of the same order of magnitude, the toughness of the matrix is not completely exploited in the composite. Further, when fracture occurs in the matrix layer, the time dependence of the fracture toughness of the composite is similar to that of the matrix. If interfacial fracture occurs, the time dependence of the matrix may not be transferred to the composite. (ii) as for the prop-

agation stage, some results on the fibre bridging mechanism and its relation to the properties of the interface between matrix and fibres were found. When the interfacial bond is weak, as it is for the composite based on the plain resin E, the energy dissipated by fibre bridging is low, although a high number of bridging fibres is observed. In the case of the toughened resin EI, the considerable increase of toughness is probably due to the energy dissipated by fracture of the matrix during crack bridging. It was verified that in this case the contribution to toughness due to the fibre bridging mechanism has the same time dependence of the fracture toughness of the matrix.

7. Acknowledgements

Authors would like to thank Arkema Company and the Groupement de Recherche du Lacq, France for the materials and the support provided and Prof. Gerald Pinter, Dr. Steffen Stelzer and the personnel of Montanuniversität of Leoben, Austria, for their help and willingness.

References

[1] A. R. Offringa, Thermoplastic compositesrapid processing applications, Compos. Part A Appl. Sci. Manuf. 27 (4) (1996) 329–336.

[2] N. Bernet, V. Michaud, P.-E. Bourban, J.-A. Månson, Commingled yarn composites for rapid processing of complex shapes, Compos. Part A Appl. Sci. Manuf. 32 (11) (2001) 1613–1626.

[3] F. Henninger, K. Friedrich, Thermoplastic filament winding with online-impregnation. Part A: process technology and operating efficiency, Compos. Part A Appl. Sci. Manuf. 33 (11) (2002) 1479–1486.

[4] P. Mitschang, M. Blinzler, A. Wöginger, Processing technologies for continuous fibre reinforced thermoplastics with novel polymer blends, Compos. Sci. Technol. 63 (14) (2003) 2099–2110.

[5] F. O. Sonmez, M. Akbulut, Process optimization of tape placement for thermoplastic composites, Compos. Part A Appl. Sci. Manuf. 38 (9) (2007) 2013–2023.

[6] H. Parton, I. Verpoest, In situ polymerization of thermoplastic composites based on cyclic oligomers, Polym. Compos. 26 (1) (2005) 60–65.

[7] K. van Rijswijk, H. Bersee, Reactive processing of textile fiber-reinforced thermoplastic composites An overview, Compos. Part A Appl. Sci. Manuf. 38 (3) (2007) 666–681.

[8] W. M. Jordan, W. L. Bradley, R. J. Moulton, Relating Resin Mechanical Properties to Composite Delamination Fracture Toughness, J. Compos. Mater. 23 (9) (1989) 923–943.

[9] R. Frassine, M. Rink, A. Pavan, Viscoelastic effects on the interlaminar fracture behaviour of thermoplastic matrix composites: II. Rate and temperature dependence in unidirectional PEEK/carbon-fibre laminates, Compos. Sci. Technol. 56 (11) (1996) 1253–1260.

[10] K. Friedrich, R. Walter, L. A. Carlsson, A. J. Smiley, J. W. Gillespie, Mechanisms for rate effects on interlaminar fracture toughness of carbon/epoxy and carbon/PEEK composites, J. Mater. Sci. 24 (9) (1989) 3387–3398.

[11] R. Frassine, A. Pavan, Viscoelastic effects on the interlaminar fracture behaviour of thermoplastic matrix composites: I. Rate and temperature dependence in unidirectional PEI/carbon-fibre laminates, Compos. Sci. Technol. 54 (2) (1995) 193–200.

[12] W. L. Bradley, Understanding the Translation of Neat Resin Toughness into Delamination Toughness in Composites, Key Eng. Mater. 37 (1989) 161–198, doi:10.4028/www.scientific.net/KEM.37.161.

[13] N. A. Siddiqui, R. S. Woo, J.-K. Kim, C. C. Leung, A. Munir, Mode I interlaminar fracture behavior and mechanical properties of CFRPs with nanoclay-filled epoxy matrix, Compos. Part A Appl. Sci. Manuf. 38 (2) (2007) 449–460.

[14] P. Compston, P.-Y. B. Jar, P. J. Burchill, K. Takahashi, The Transfer of Matrix Toughness to Composite Mode I Interlaminar Fracture Toughness in Glass-Fibre/vinyl Ester Composites, Appl. Compos. Mater. 9 (5) (2002) 291–314.

[15] S. A. Ngah, A. C. Taylor, Toughening performance of glass fibre composites with coreshell rubber and silica nanoparticle modified matrices, Compos. Part A Appl. Sci. Manuf. 80 (2016) 292–303.

[16] T. Pini, F. Briatico-Vangosa, R. Frassine, M. Rink, Fracture toughness of acrylic resins: viscoelastic effects and deformation mechanisms, Polym. Eng. Sci. Accepted for publication.

[17] ISO 15024, Fibre-reinforced plastic composites - Determination of mode I interlaminar fracture toughness, GIc, for unidirectionally reinforced materials, Tech. Rep. 15024, International Organization for Standardization, Geneva, CH, 2001.

[18] E. Greenhalgh, Failure analysis and fractography of polymer composites, Elsevier, 2009.

Table 1: Logarithms of shift factors ($\mathrm{Log}(a_{23}^{T})$) at different temperatures for both matrices.

	0 °C	23 °C	40 °C	60 °C
E matrix	0.39	0	-0.81	-1.64
EI matrix	2.52	0	-1.55	-4.02

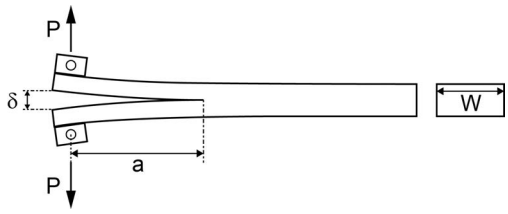

Figure 1: Double cantilever beam test configuration.

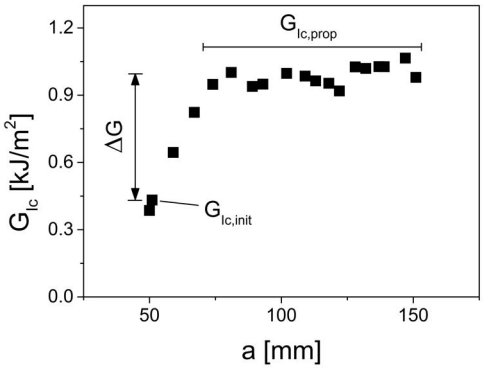

Figure 2: Fracture toughness, G_{Ic}, vs. crack length, a, at 23 °C and 20 mm/min for E composite.

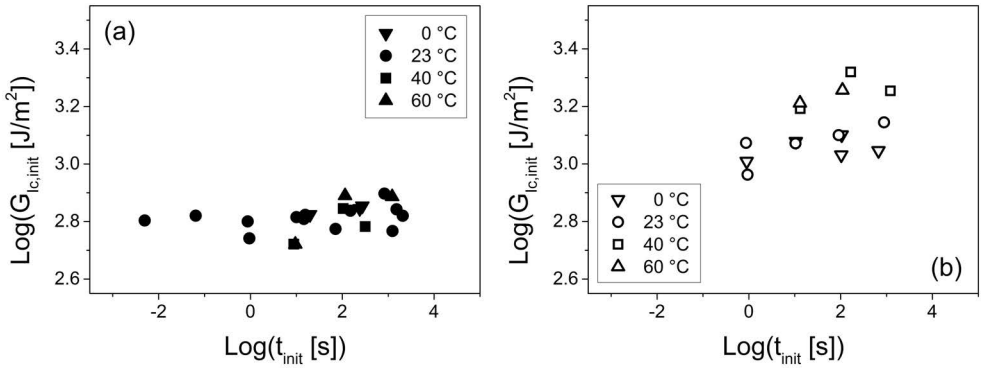

Figure 3: Fracture toughness, $G_{Ic,init}$, vs. crack initiation time, t_{init}, isothermal curves for E (a) and EI composite (b).

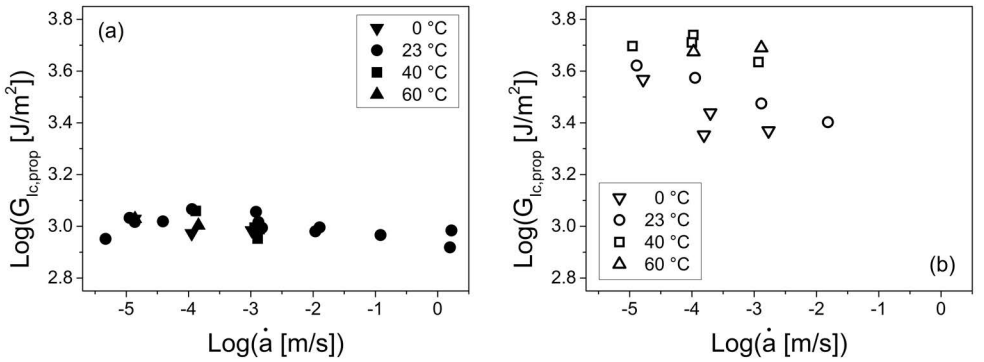

Figure 4: Fracture toughness, $G_{Ic,prop}$, vs. crack propagation speed, $\dot{a}$, isothermal curves for E (a) and EI composite (b).

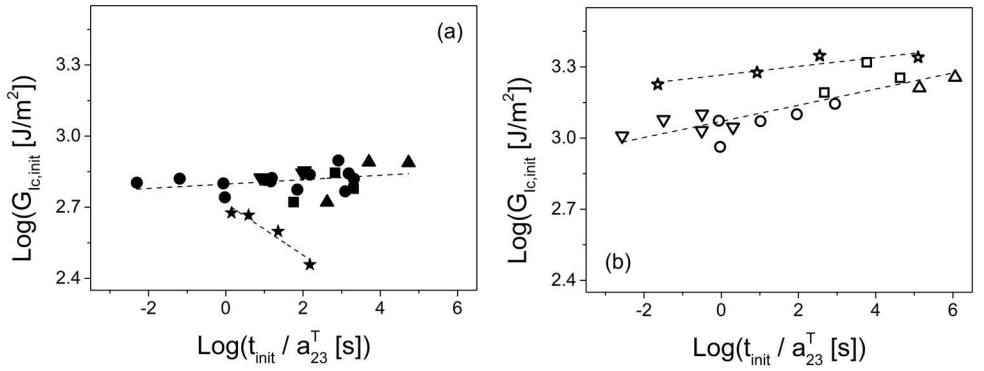

Figure 5: Fracture toughness, $G_{Ic,init}$, vs. crack initiation time, t_{init}, master curves for composites (same symbols used in Fig. 3) and matrices (stars) at the reference temperature of 23 °C for E (a) and EI resins (b). Dashed lines are a visual aid.

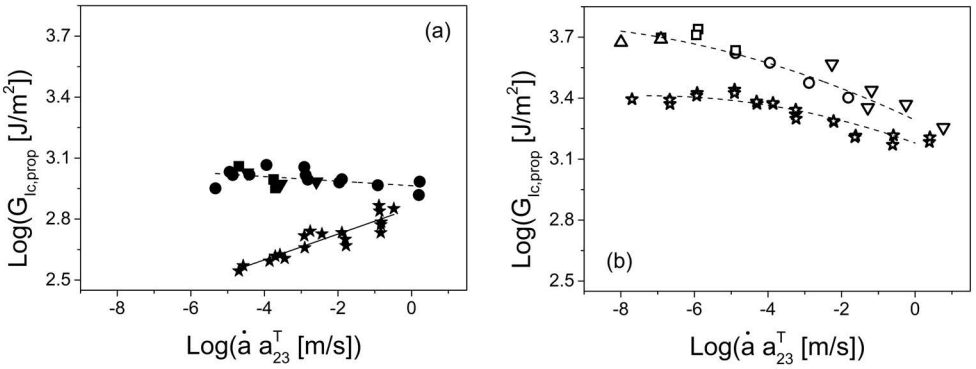

Figure 6: Fracture toughness, $G_{Ic,prop}$, vs. crack propagation speed, $\dot{a}$, master curves for composites (same symbols used in Fig. 4) and matrices (stars) at the reference temperature of 23 °C for E (a) and EI resins (b). Solid line is a power law fitting, dashed lines are a visual aid.

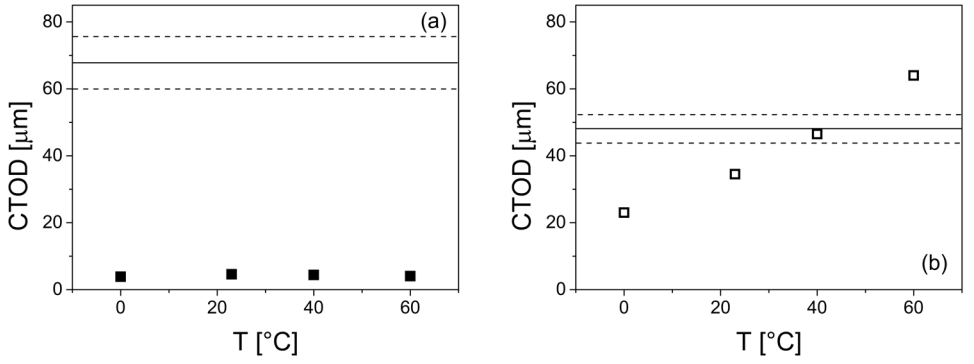

Figure 7: Crack tip opening displacement, CTOD, of bulk matrices as a function of temperature for E (a) and EI matrix (b). Solid and dashed lines represent the average value and standard deviation of thickness of the interlaminar resin-rich layer for E (a) and EI composite (b) respectively.

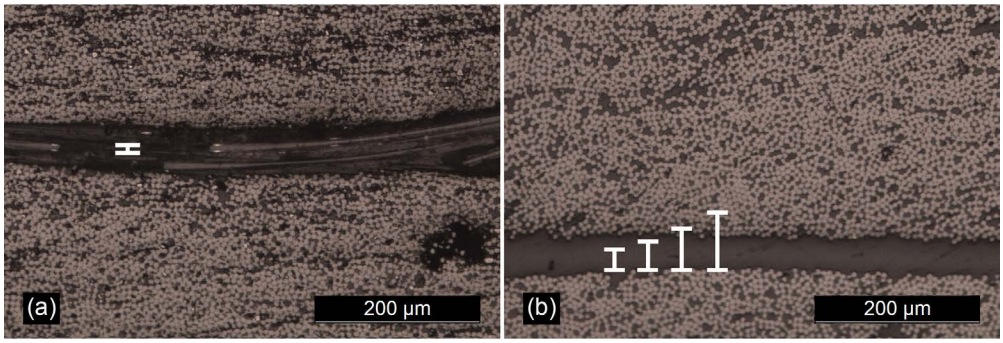

Figure 8: Cross-section of E (a) and EI composite (b). The dark area is the resin-rich region on which the CTOD (average of the values from Fig. 7 (a)) of E matrix (a) and CTOD (values from Fig. 7 (b)) of EI matrix (b) are reported.

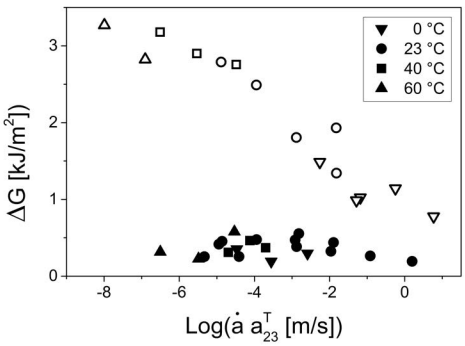

Figure 9: ΔG ($G_{Ic,prop} - G_{Ic,init}$) vs. crack initiation time, t_{init}, for E (solid symbols) and EI composite (open symbols).

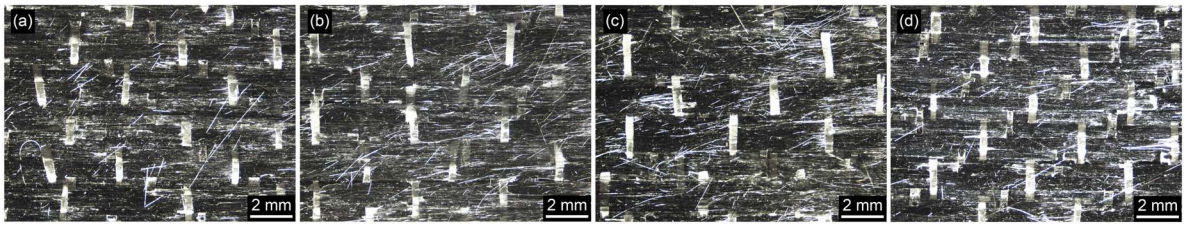

Figure 10: Fracture surfaces of E composite tested at 2 mm/min, 0 °C (a), 23 °C (b), 40 °C (c) and 60 °C (d).

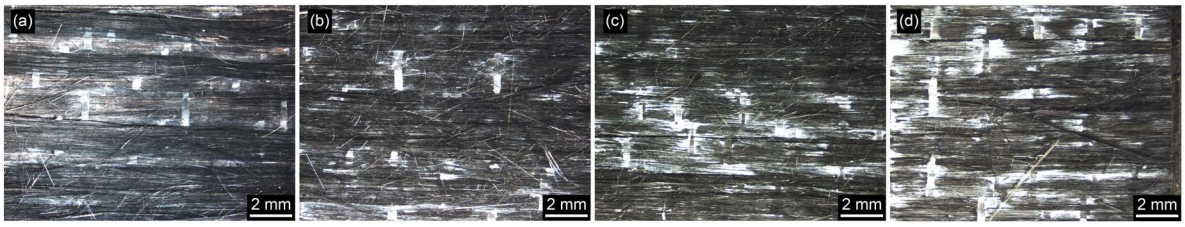

Figure 11: Fracture surfaces of EI composite tested at 2 mm/min, 0 °C (a), 23 °C (b), 40 °C (c) and 60 °C (d).

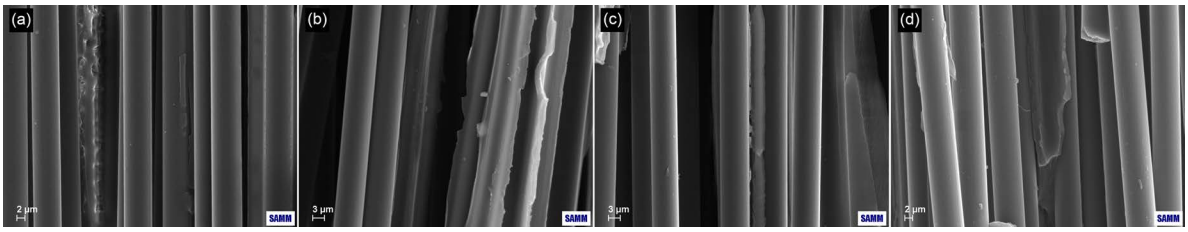

Figure 12: SEM images of fracture surfaces of E composite tested at 20 mm/min, 0 °C (a), 23 °C (b), 40 °C (c) and 60 °C (d). Magnification 5000x.

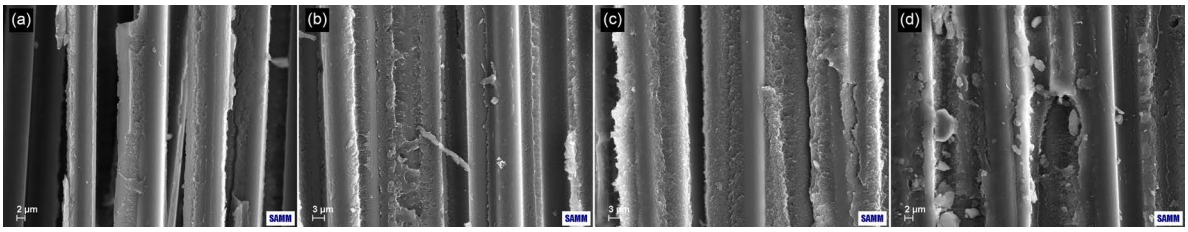

Figure 13: SEM images of fracture surfaces of EI composite tested at 20 mm/min, 0 °C (a), 23 °C (b), 40 °C (c) and 60 °C (d). Magnification 5000x.

List of Tables

List of Figures